ELSEVIER

Polymer 44 (2003) 2321–2329

polymer

www.elsevier.com/locate/polymer

Towards the simulation of poly(vinyl phenol)/poly(vinyl methyl ether) blends by atomistic molecular modelling

Patricia Gestoso, Josée Brisson*

CERSIM, Département de chimie, Faculté de sciences et de génie, Université Laval, Québec, Qué., Canada G1K 7P4

Received 17 September 2002; received in revised form 21 January 2003; accepted 23 January 2003

Abstract

Molecular simulations of poly(vinyl phenol)/poly(vinyl methyl ether) (PVPh/PVME) blends were performed and their degree of miscibility evaluated as a preliminary step before orientation simulations. A minimum of three periodic boundary condition amorphous models was constructed and analysed in terms of solubility parameter, X-ray pattern, pair correlation function, hydrogen bond fraction and backbone conformation. The values obtained are consistent with miscibility of the systems, although it is suggested that the degree of mixing is not uniform for the different models.

Keywords: Atomistic simulation; Polymer blends; Hydrogen bonding

1. Introduction

Blending is an interesting alternative to synthesis to obtain new polymeric materials, as it is usually easier, faster and less expensive. Nevertheless, although one expects properties to be intermediate to those of the pure components, this is not always the case. This is particularly striking in the case of orientation, as a maximum in the orientation for both poly(vinyl methyl ether) (PVME) and poly(4-vinyl phenol) (PVPh) is observed around 50 mol% composition [1]. Hence the interest in modelling these blends and, eventually, their behaviour upon deformation.

Blend modelling can and has been pursued with two main objectives: prediction of miscibility and/or of miscible blend properties. Although not mutually exclusive, the objective will inevitably affect choice of method used to perform the modelling.

Construction of blend models has been directed mostly to homopolymer blends, such as the coarse models used for studying polymer dynamics more realistically [2–5]. In such cases, focus was put mostly on polymer property calculations. Attempts to model blends containing chemically different polymers have been mainly restricted to short chains, as in the work of Doxastakis et al. [6], where segmental relaxation functions were calculated for a blend of seven chains of 16-mer *cis*-1,4 polyisoprene with three chains of 20-mer 1,2 polybutadiene using molecular dynamics. Among the few studies featuring long chain blends, one of the first was from Choi et al. [7], who have studied the immiscibility of poly(ethylene) (PE) and poly(propylene) (PP). The authors found that chains of the different polymers segregate into distinct domains even when the initial state was highly interpenetrated. Recently, Mattice and coworkers [8,9] have used Monte Carlo simulations with a coarse-grained representations of the chains to model PE/PP blends [9] and mixtures of PP chains with different stereochemical compositions [8]. In these cases, focus is put on miscibility predictions, and the authors use intermolecular pair correlations and visual inspection of the cells after equilibration to establish the miscibility behaviour of the systems.

In this article, a blend for which miscibility is clearly established experimentally was used. Miscibility predictions will therefore not be one of the aims sought. We present a first attempt to construct two PVPh/PVME blends with different compositions. PVME structures have also been built for comparison purposes. Several parameters have been calculated for the systems in order to investigate the degree of miscibility attained in the model constructed, while supposing that the blends are, in reality, miscible at the molecular level, as is expected from experimental data

* Corresponding author. Tel.: +1-418-656-3536; fax: +1-418-656-7916.
E-mail address: jbrisson@chm.ulaval.ca (J. Brisson).

0032-3861/03/$ - see front matter © 2003 Elsevier Science Ltd. All rights reserved.
doi:10.1016/S0032-3861(03)00098-3

available [10]. The results are compared to those reported from experiments in the literature, when available. The usefulness of these parameters for assessing the degree of intermingling or miscibility at the molecular level is also discussed.

2. Methodology

2.1. Experimental

Poly(vinyl phenol) of molecular weight of 29,300 g mol^{-1} was purchased from TriQuest. Poly(vinyl methyl ether) from Aldrich had a molecular weight of 111,000 g mol^{-1}. Preparation of PVPh/PVME blends was done by solution in acetone. Details are provided elsewhere [1].

X-ray diffraction patterns were recorded on a Rigaku X-ray spectrometer type 200B rotating anode generator functioning at 180 mA and 45 kV using the Ni filtered copper Kα radiation. Spectra were recorded in the θ–2θ geometry.

2.2. Model construction and validation

Molecular modelling was performed using the InsightII, Polymerizer, Amorphous_Cell and Discover 3 software packages of Accelrys Inc., installed on a Indigo II Silicon Graphics workstation and on an SGI Origin2000 processor. The polymer consistent forcefield (PCFF) [11–13] was used throughout.

Construction of the poly(vinyl phenol) (PVPh) models has been described elsewhere [14]. These consisted in a single parent chain of atactic PVPh with 250 repeat units, setting the probability of *meso* dyads at 0.5. Atactic poly(vinyl methyl ether) (PVME) models were constructed as a single chain of 250 repeat units using a random dihedral angle distribution. In order to improve the quality of initially generated structures, the use of five substates of 20 degrees were allowed. In addition, each new bond was incorporated taking into account six lookahead bonds, an option that reduces the occurrence of high energy models.

Two poly(vinyl phenol)/poly(vinyl methyl ether) (PVPh/PVME) blends with different compositions were constructed. Blends referred to as PP55 were composed of one chain of atactic PVPh and one chain of atactic PVME, each one with 250 repeat units ($M_w = 30,000$ g mol^{-1} and $M_w = 14,500$ g mol^{-1}, respectively). PP55 system has 50% PVPh molar content (67 wt% of PVPh). A second system, referred to as PP37, contains one chain of atactic PVPh and two chains of atactic PVME. Again, each chain has 250 repeat units. This blend has a 33% molar content of PVPh, corresponding to 51 wt% of PVPh.

For all models, chains were constructed unit by unit. For the blends, the construction of the models was done simulating step growth polymerization. First, a PVPh repetitive unit was placed into the cell, which was followed by placing a repetitive unit of PVME randomly into the same cell. Segments of PVPh and PVME were incorporated alternatively to PVPh and PVME chains until desired molecular weight was reached. In the case of the PP37 blends, one PVPh chain and two PVME chains were constructed simultaneously: One segment of the correspondent repetitive unit was added to each one of the three chains successively. In all cases, in order to reduce the occurrence of high energy configurations, six lookahead bonds were taken into account while adding each unit to the chains under construction. Five substates of 40 degrees width were used, in the aim of ensuring more uniform filling of the available space and of decreasing the probabilities of accidentally generating arrangements in which two atoms overlap [15]. To limit catenation problems, the blends were constructed at an initial density of 0.5 g cm^{-3} and were compressed to attain the desired density at 298 K. PVPh density was experimentally obtained previously, its value being equal to 1.25 g cm^{-3}. PVME density was calculated using an empirical expression as a function of temperature, developed for this polymer in the literature [16], which led to a value of 1.058 g cm^{-3} at 298 K. Densities of PP55 and PP37 blends were calculated using a weight average over the pure component densities. PP55 and PP37 densities were fixed as 1.19 and 1.154 g cm^{-3}, respectively. An auto-ring-checking procedure was used to reject models presenting catenation during their construction. The resulting cubic cells had a side of 34.17 Å (PVPh), 28.35 Å (PVME), 40.03 Å (PP55) and 43.52 Å (PP37). All simulations reported here were performed under periodic boundary conditions.

Using the method described above, three amorphous structures with different conformations were successfully generated for PVPh, PVME and PP55 blends. For PP37 blends, as more chains were involved, four structures were constructed to obtain a more representative sampling. For all the blend models constructed the different chains were in contact and, visually, a good degree of interpenetration could be detected. In order to verify if interpenetration could be improved, a star copolymer representing PP55 composition (two branches of PVPh and two branches of PVME) was constructed. The interpenetration between PVPh and PVME branches did not appear visually to have changed, and various parameters calculated were, within experimental error, unchanged with respect to the previously built models described above.

After initial cell construction, an annealing procedure was applied to the cells. Structures were equilibrated at 1000 K for 5 ps using an integration step of 0.001 ps and the Verlet velocity algorithm under the microcanonical (NVT) ensemble. A cutoff distance of 9.5 and a buffer of 0.5 Å was fixed to limit calculation time for nonbonded interactions. This was followed by a coarse energy minimization using the steepest descent algorithm until derivatives were less than 0.1 kcal mol^{-1}. Finally, the conjugate gradients energy

minimization method was applied, allowing a maximum deviation of energy derivatives of 0.1 kcal mol^{-1}. It must be noted that this procedure did not allow the system to visit all possible states, and therefore does not permit prediction of miscibility of the systems. Fig. 1 shows typical examples of PP55 and PP37 models.

Tables 1–3 show total potential energy and its various components for the different minimized structures. For PVME and PP55, energy terms were similar for the three models, confirming that these structures are satisfactorily relaxed. For PP37 blends, model 4 exhibits a markedly different electrostatic term and, hence, global energy.

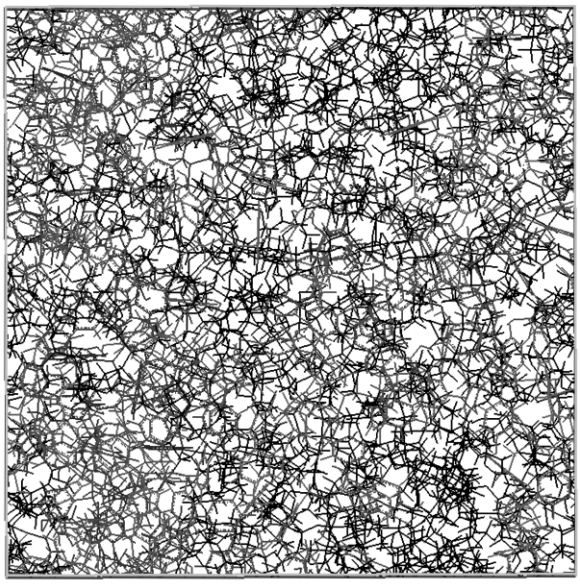

(a)

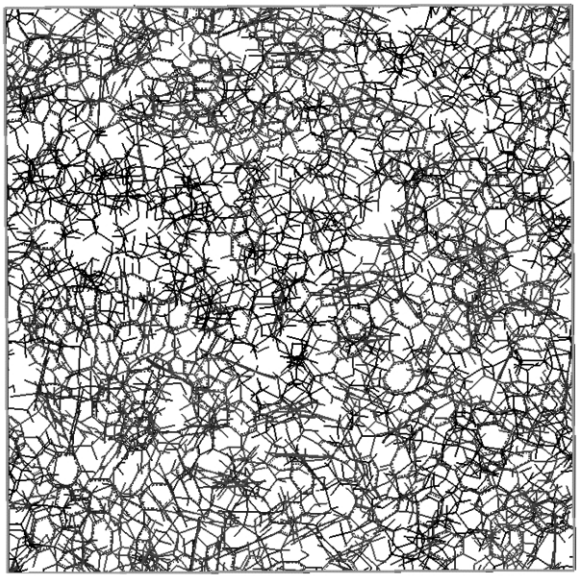

(b)

Fig. 1. Periodic amorphous cell packing of representative blends (PVPh chains in gray, PVME chains in black) (a) PP55, model 1 (b) PP37, model 1.

Table 1
Minimization energy (kcal mol^{-1}) summary for poly(vinyl methyl ether)

Component	Model 1	Model 2	Model 3
Total potential energy	−1362	−1335	−1362
Internal	−835	−814	−848
Bond	97	96	94
Angle	1011	985	1012
Torsion	−1506	−1463	−1516
Out-of-plane	0	0	0
Cross	−437	−432	−439
Nonbond	−527	−522	−514
van der Waals (vdW)	−527	−522	−514
vdW_repulsive	6646	6685	6652
vdW_dispersive	−7173	−7207	−7166
Electrostatic	0	0	0

A hydrogen bond was considered to be formed when the distance between the hydrogen donor and the oxygen acceptor was less than 3.0 Å and the angle between the proton acceptor, the proton and the proton donor was greater than 90 degrees [14]. Three types of hydrogen bonds were considered for the O–H groups of the parent PVPh chain: those with oxygen acceptors belonging to the parent chain (intrachain PVPh–PVPh hydrogen bonds), those with oxygen acceptors belonging to the surrounding PVPh chain replicates (interchain PVPh–PVPh hydrogen bonds) and those with oxygen acceptors belonging to the PVME chains (interchain PVPh–PVME hydrogen bonds). Whereas InsightII was used to determine intrachain hydrogen bonds, other hydrogen bonds were calculated using a subroutine written by the authors.

Calculated error, when reported, corresponds to that estimated using the Student test on the various models considered, with a probability level of 95%.

3. Results and discussion

The miscibility of PVPh/PVME blends has been clearly established in the literature, and various experimental data

Table 2
Minimization energy (kcal mol^{-1}) summary for poly(vinyl phenol phenol)/poly(vinyl methyl ether) 50:50 (PP55)

Component	Model 1	Model 2	Model 3
Total potential energy	−8110	−8187	−8224
Internal	−1661	−1713	−1730
Bond	745	744	733
Angle	2085	2058	2013
Torsion	−3033	−3067	−3044
Out-of-plane	9	9	8
Cross	−1467	−1457	−1440
Nonbond	−6449	−6473	−6494
van der Waals (vdW)	−682	−717	−701
vdW_repulsive	20664	20615	20592
vdW_dispersive	−21347	−21333	−21294
Electrostatic	−5767	−5756	−5792

Table 3
Minimization energy (kcal mol^{-1}) summary for poly(vinyl phenol)/poly (vinyl methyl ether) 33:67 (PP37)

Component	Model 1	Model 2	Model 3	Model 4
Total potential energy	−7741	−7924	−7767	−10862
Internal	−2346	−2445	−2381	−2466
Bond	863	842	851	803
Angle	3209	3075	3188	3174
Torsion	−4476	−4461	−4489	−4489
Out-of-plane	10	9	10	9
Cross	−1953	−1910	−1940	−1963
Nonbond	−5395	−5479	−5385	−8396
van der Waals (vdW)	−1241	−1255	−1262	−1269
vdW_repulsive	29230	29177	29123	27919
vdW_dispersive	−30471	−30432	−30385	−29188
Electrostatic	−4154	−4224	−4123	−7127

point to a miscibility at the molecular level [1,10]. The present modelling study therefore aims at providing suitable representations for the real systems, which can be evaluated by comparing with experimental data. In the present work, solubility parameter, X-ray pattern and number of hydrogen bonds were evaluated to estimate the validity of the models. Further, pair correlation functions and conformation distribution were analysed, as these give insights on the degree of intermingling and on the effect of blending on the overall organisation of the polymer.

3.1. Cohesive energy and solubility parameter

Cohesive energy is a widely used criterion to determine if the cell structure and the forcefield chosen describe properly the real material. The cohesive energy density (e_{coh}) is defined as the increase in energy per mole of a material if all intramolecular forces are eliminated, i.e.

$$e_{coh} = (E_{coh}/V) \quad (1)$$

where E_{coh}, the cohesive energy, is calculated as the difference in the potential energies between the isolated chain and the parent chains in the bulk, and V is the volume of the amorphous cell. The square root of the cohesive energy density is the solubility parameter δ, which describes the attractive strength between the molecules of the material.

The simulated solubility parameter values for the different conformations of PVPh, PVME, PP55 and PP37 are shown in Table 4. As determined previously [14], solubility parameter for PVPh agrees with the lower experimental value reported in the literature (9.5(cal cm^{-3})$^{1/2}$), but is inferior to the upper value reported of 11.7 (cal cm^{-3})$^{1/2}$ [17]. On the other hand, simulation values for PVME are within results reported from chemical group contribution techniques, which lead to values from 8.15 to 9.61 (cal cm^{-3})$^{1/2}$ [18]. It is proposed that the better reproducibility in the case of PVME is related to the absence

Table 4
Simulated solubility parameter ((cal cm^{-3})$^{1/2}$)

System	Model	δ	Average δ
PVPh [14]			8.7 ± 1.2
PVME	1	8.3	8.4 ± 0.2
	2	8.4	
	3	8.5	
PP55	1	8.7	8.4 ± 0.8
	2	8.3	
	3	8.1	
PP37	1	8.7	8.7 ± 0.5
	2	8.2	
	3	8.7	
	4	9.0	

Each value pertains to one of the two chains present in the model.

of strong intra and interchain interactions for this polymer when compared to with PVPh.

In general, if two different polymers have similar values of δ, they will tend to be mutually soluble, the critical value of the solubility parameter difference ($\Delta\delta$) between pure components being around 0.3–0.5 (cal cm^{-3})$^{1/2}$ [19]. As the difference for simulation data is of 0.3 ± 1.2 (cal cm^{-3})$^{1/2}$, the solubility parameters obtained from the simulations are in agreement with the experimentally observed miscibility.

The solubility parameter of a mixture is often taken as the sum of the solubility parameters of the respective pure components, averaged over the volume [20]. If using the values obtained from simulation for the pure components, this would lead to values of 8.6 and 8.5 (cal cm^{-3})$^{1/2}$ for PP55 and PP37, respectively, which agree with those from simulations, within the observed data dispersion. On the other hand, it should be stressed that the solubility parameter difference ($\Delta\delta$) between pure components and blends is of the same order of magnitude as that of the data dispersion. Therefore, although the results show that the simulated models respect the established rules for miscibility, the solubility parameters cannot be relied upon to verify the correctness of the miscible blend models.

Nevertheless, the fact that the solubility parameters of blends and pure polymers are close to one another suggests that the intramolecular forces are not changing dramatically upon blending, PVME chains replacing PVPh chains with little change in the cohesion between molecules forming the material. Further, solubility values do not vary substantially between the different models constructed for a same composition. This indicates that this parameter may not be very sensitive to conformation and homogeneity differences at a molecular level.

3.2. X-ray pattern

Experimental and calculated X-ray diffraction spectra for PVME and PP55 and PP37 blends are shown in Fig. 2. The intensity values are presented on a relative scale for

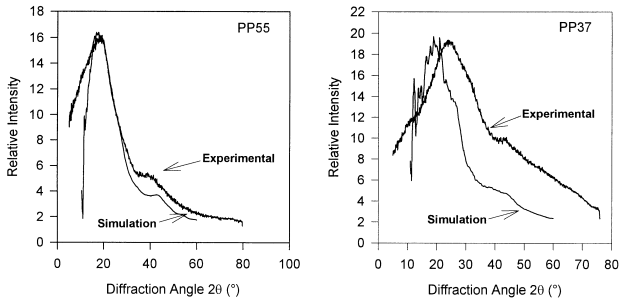

Fig. 2. Comparison between X-ray patterns for experimental samples and simulation for a typical PP55 and PP37 blends (Model 1 represented).

comparison purposes. The calculated spectra pertain to models labelled 1 for PVME, PP55 and PP37. In all cases, these are representative of the general tendency observed in all models. It can be seen that, for both blends, the position of the typical amorphous halos at 20 and 42 degrees are reproduced by the models. Deviations could be related to differences in polydispersity, tacticity and stereoregularity between experimental samples and simulation models. Further, the model calculations are performed on a single model, and the commercial package used for the simulations/calculations did not include the implementation of thermal factors for amorphous polymer systems. Therefore, differences in thermal agitation between the two blends are not modelled. These are proposed to account for the larger width of the scattering peaks observed experimentally for both polymers. In addition, the glass transition temperature is quite different for both blends modelled, the experimental onset temperature for the glass transition T_g for PP37 (57 °C) being closer to room temperature than that of PP55 (101 °C). Thermal agitation is therefore expected to be more important for PP37, which accounts for the experimental increase in width for this blend as compared to PP55, and which also accounts for this difference in width not being observed in the model calculations. The general shape of the spectra, either experimental or simulated, are however in agreement with those reported for pure PVPh in a previous article [14]. Once again, X-Ray patterns simulation does not seem to afford insights on the degree of intermingling of the chains.

3.3. Pair correlation function

The regularity of the cell can also be characterised using the pair correlation function, $g(r)$, for each pair of atoms. This function represents the probability of finding a pair of atoms in the system at a distance r apart relative to the probabilities expected for a completely random distribution at the same density. The $g(r)$ function can be separated in two main contributions: The intramolecular radial distribution function, which includes all correlations between atoms on the same chain, and the intermolecular radial distribution function, which is related to the molecular arrangement in the bulk structure and accounts for correlations only among atoms on different chains [21]. The reproduction of a reliable $g(r)$ by a simulation can be used as a measure of the reliability of the forcefield [13], as well as to assess miscibility [8,9].

Fig. 3 shows the intramolecular distribution for the carbon-carbon pairs for pure PVPh [14], pure PVME as well as PVPh and PVME in model 1 of the PP37 blend (analogous plots for PP55 blends, not reported, show the same tendencies as those calculated for PP37 blends). For pure PVME, strong peaks near 1–1.75 Å can be observed, related to atom connectivity. The presence of atomic pairs without connectivity in the spatial vicinity are responsible of the peaks around 2–4 Å. For values of $r > 4$ Å, $g(r)$ tends towards 0, which indicates that no long-range order exists inside the cell. When observing the intramolecular distribution for PVPh and PVME in the PP37 blends, no significant changes are noticed. This behaviour is expected, since intramolecular short-distances are not supposed to be affected by the presence of another polymer. In addition, the Figure allows to conclude that other distinct polymer chains do not establish a long-range order inside the cell.

Recently, Mattice et al. [8,9] have used a comparison between different components of the intermolecular distribution function $g(r)$ to assess miscibility. When $g(r)$ values for atom pairs belonging to distinct components are higher than those obtained for pairs in the individual homopolymers, they proposed that the blend shows a tendency towards miscibility: the difference between values is proposed to be due to inter-homopolymer contacts being favored over intra-homopolymer contacts. The opposite behaviour, higher values of $g(r)$ for pairs belonging to a same homopolymer, is seen as an indication of immiscibility at molecular level.

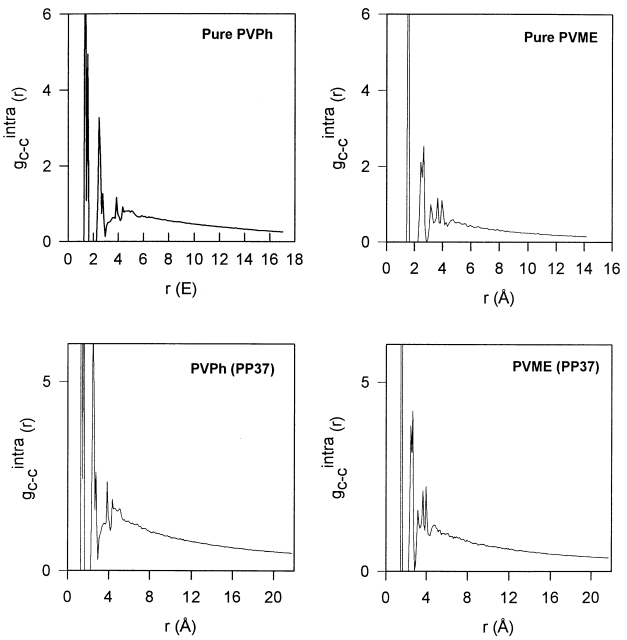

Fig. 3. Intramolecular distribution for the carbon-carbon pairs for PVPh [14] and PVME, pure and in PP37 blends (Model 1 represented).

Carbon–carbon distributions for PVPh–PVPh, PVME–PVME and PVPh–PVME pairs for PP55 and PP37 blends are plotted in Fig. 4. The curves were calculated as the average for the different conformations with the exception of the PVPh–PVPh intermolecular pair correlation function for PP37, for which the curve of model 2 was excluded as it presented an abnormally low behaviour. First, whereas $g(r)$ reaches 1 for PVPh–PVME pairs, for homopolymer pairs the convergence to 1 is much slower. This is attributed to the limited size of the blend models, which may limit their validity. In-progress simulations on polyisoprene/polybutadiene blends carried out by varying the box size show that this failure of reaching 1 for blends is a size effect, disappearing when using bigger simulation boxes [22]. Nevertheless, it should be pointed that those simulations also indicate that at the same r distance, the $g(r)$ pattern obtained for small and big boxes follows the same tendency. Therefore, although some of the $g(r)$ curves do not reach 1, the conclusions about miscibility obtained by our models are still valid.

No sharp peaks are observed in the plots of Fig. 4. This indicates that two atoms of two different molecules are not systematically at a r distance from one another, which is consistent with the absence of crystalline-like order. For the PP55 blends, the intermolecular pattern for the cross interactions (PVPh–PVME) is higher that for carbon–carbon atoms belonging to the same homopolymer. This indicates that PVPh and PVME atoms are preferentially surrounded by PVME and PVPh atoms, respectively, instead of by segments of their own homopolymers. This is a strong indicator of tendency towards miscibility. Nevertheless, $g(r)$ for PVME–PVME contacts is higher than for PVPh–PVPh. This difference can be attributed to the side group of PVME being less bulky that the phenol side group of PVPh, so the approach between PVME carbon atoms of different chains is sterically more favoured.

For PP37 blends, again the $g(r)$ for the PVPh–PVME contacts is higher than for the one-component contacts, suggesting also miscibility in these models. However, although the PVPh–PVME $g(r)$ curve presents the highest values, they are very similar, at small distances, to those of the PVME–PVME $g(r)$ distribution. The similarity between

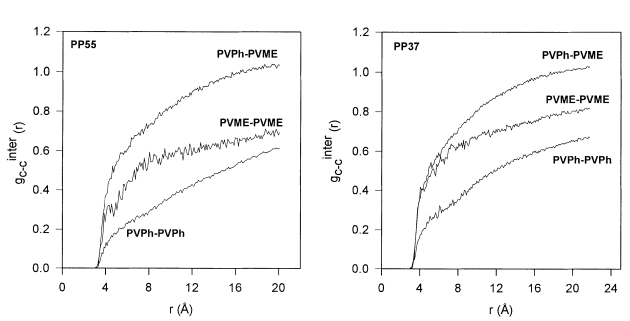

Fig. 4. Intermolecular distribution for the carbon-carbon pairs in PP55 and PP37 blends (average for all models represented, all carbons used for the calculations).

both curves can partly be due to the predominance of PVME in the blend (two molecules of PVME are present for each chain of PVPh), which leads to a higher percentage of possible contacts between PVME atoms when compared to the PP55 blend.

As, in the present case, the interactions which lead to miscibility are hydrogen bonds, pair distribution calculations of oxygen–oxygen atom pairs can provide useful insights on the degree of intermingling. These will be discussed, in conjunction with calculation of the number of hydrogen bonds, in Section 3.4.

3.4. Hydrogen bonding

One of the most interesting aspects of PVPh and its blends, for which these were chosen as model systems in the first place, is the formation of interchain hydrogen bonds they exhibit. These are amenable to FTIR characterisation, and although quantification has not been reported for the PVPh–PVME system, it is known that a non-negligible fraction of PVPh–PVME hydrogen bonds occurs in the miscible blend. Moskala et al. [10] have reported that total hydrogen bond fraction increases with PVME content, the intensity of the bonded hydroxyl vibration increasing in detriment of the free hydroxyl vibration. Table 5 shows the percentage of free and bonded hydroxyls for PVPh [14] and PVPh/PVME blends. In the last column it can be seen that the total percentage of hydrogen bonds does not change with blending, being around 60% for pure PVPh as well as for the blends. The simulation value for pure PVPh is in excellent agreement with the semi-quantitative measurements reported by our group, which estimated that 59% of hydroxyl groups form hydrogen bonds [23]. Intrachain, interchain PVPh–PVPh and interchain PVPh–PVME hydrogen bond percentages were also calculated. Whereas the interchain PVPh–PVPh fraction does not change appreciably, intrachain bonds decrease by around 10% upon blending, irrespective of PVME composition. On the other hand, interchain PVPh–PVME bond percentages increase with PVME composition. Therefore, it is suggested that part of the intrachain bonds formed between PVPh chains disappear in favour of PVPh–PVME bonds.

The fact that intrachain bonds decrease and interchain PVPh–PVME bonds increase in blends when compared to pure PVPh confirms that, during the construction and subsequent relaxation of the blend, PVPh is interpenetrated with PVME chains, decreasing intrachain PVPh–PVPh contacts and exposing more segments to PVME neighbouring chains.

The values corresponding to the PP37 blend show that, in the case of interchain PVPh–PVME hydrogen bonds, there is a substantial increase for model 4 when compared to the other three models. This difference confirms that there is an important variation between the different models when compared to PP55 blends. This is tentatively attributed to the higher number of chains involved in the construction

Table 5
Hydrogen bond distribution

System	Model	Intrachain PVPh–PVPh	Intrachain PVPh–PVPh average (%)	Interchain PVPh–PVPh	Interchain PVPh–PVPh average (%)	Interchain PVPh–PVME	Interchain PVPh–PVME average (%)	Total	Total average (%)
PVPh [14]			40 ± 20		20 ± 20				60 ± 10
PP55	1	25.2	28 ± 7	22.0	18 ± 9	10.4	15 ± 20	57.6	61 ± 20
	2	30.4		14.8		9.6		54.8	
	3	29.2		16.8		24.4		70.4	
PP37	1	26.0	29 ± 20	15.2	15 ± 7	11.6	18 ± 20	52.8	62 ± 20
	2	43.6		8.4		8.4		60.4	
	3	26.8		18.8		8.8		54.4	
	4	21.2		16.0		41.6		78.8	

(three) which increases the possibilities of valid arrangements for creating a low energy model. It is noteworthy that this model had a lower energy (see Table 3), and more specifically a lower electrostatic energy. The higher quantity of interchain hydrogen bonds (more than the double) could therefore explain the lower electrostatic energy values observed for this model when compared to the other three models. Nevertheless, it did not show better blending as estimated via the $g(r)$ functions.

In Figs. 5 and 6 are presented the pair correlation functions for the oxygen atoms, which are liable to take part in hydrogen bonds. As can be seen in the Figures, such interactions manifest themselves through the appearance of a sharp peak near 3 Å, which varies in intensity with blend composition which appear in $g^{\text{intra}}_{\text{O-O}}(r)$ as well as in in $g^{\text{inter}}_{\text{O-O}}(r)$ for PVPh vs PVPh and PVPh vs PVME. It is absent from PVME vs PVME, as expected from the lack of hydrogen atom liable to form hydrogen bonds in PVME alone.

The size of this peak is indicative of the number of hydrogen bonds present in the respective model. The $g^{\text{intra}}_{\text{O-O}}(r)$ reported in Fig. 5 can be associated to the intrachain PVPh–PVPh hydrogen bonds which appear in Table 5. A good fit is found for the two blends, the lowest intensity peak for PP55 observed for model 1, which also exhibited the lowest number of hydrogen bonds (25.2% as compared to 29.2 and 30.4% for the two other models). The $g^{\text{inter}}_{\text{O-O}}(r)$ reported in Fig. 6 can be associated with interchain PVPh–PVPh and interchain PVPh–PVME values found in Table 5.

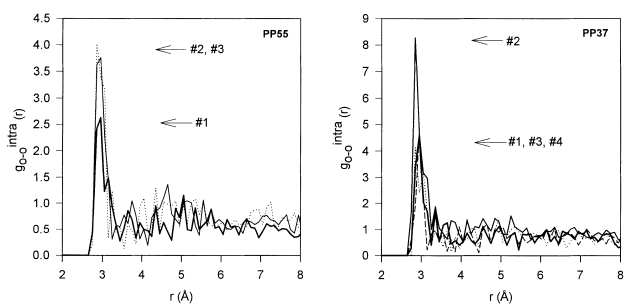

Fig. 5. Intramolecular distribution for the oxygen-oxygen pairs in PP55 and PP37 blends (thick line: Model 1, thin line: Model 2, dotted line: Model 3, dashed line: Model 4).

Again, a good agreement is found between the two different representations, with, for instance, a significantly higher peak for model 1 of PP55 for the PVPh–PVPh interactions which corresponded to a value of 22.0% with respect to values of 14.8 and 16.8% for the two other models in Table 5. For interchain PVPh–PVME interactions, similar fits are observed, with model 3 having a considerably higher peak in Fig. 6 and a higher number of hydrogen bonds (24.4% vs 9.6 and 10.4%) in Table 5. Again, similar fits can be found for PP37. Therefore, pair correlation functions afford a rapid, visual estimation of hydrogen bonds, which can be quantitatively estimated via distance and geometry calculations.

The results for the different hydroxyl fractions and oxygen pair distribution functions confirm that the constructed blend models present a good degree of miscibility, PVPh and PVME segments being close enough to form interchain hydrogen bonds. Nevertheless, the differences with experimental results and the variability in the values observed between the models indicate that the models are not homogeneous.

3.5. Conformational analysis of the amorphous models

One of the indicators that the models represent satisfactorily the real systems is the conformational distribution. Table 6 shows initial conformations for PVPh [14], PVME and the two PVPh/PVME blends, where *trans* is defined as 180 ± 30°, *gauche* ±60 ± 30° and non-*trans*, non-*gauche* ±120 ± 30° and 0 ± 30°.

In general, conformations for pure PVPh and PVME are

Table 6
Simulated conformation distribution percentages

Model	*Gauche*	*N-trans, n-gauche*	*Trans*
PVPh [14]	41 ± 5	17 ± 5	41 ± 5
PVME	44 ± 4	11 ± 7	45 ± 10
PP55	PVPh 38 ± 5	PVPh 21 ± 4	PVPh 41 ± 2
	PVME 43 ± 5	PVME 14 ± 7	PVME 43 ± 5
PP37	PVPh 40 ± 2	PVPh 20 ± 1	PVPh 41 ± 2
	PVME 44 ± 2	PVME 13 ± 1	PVME 44 ± 2

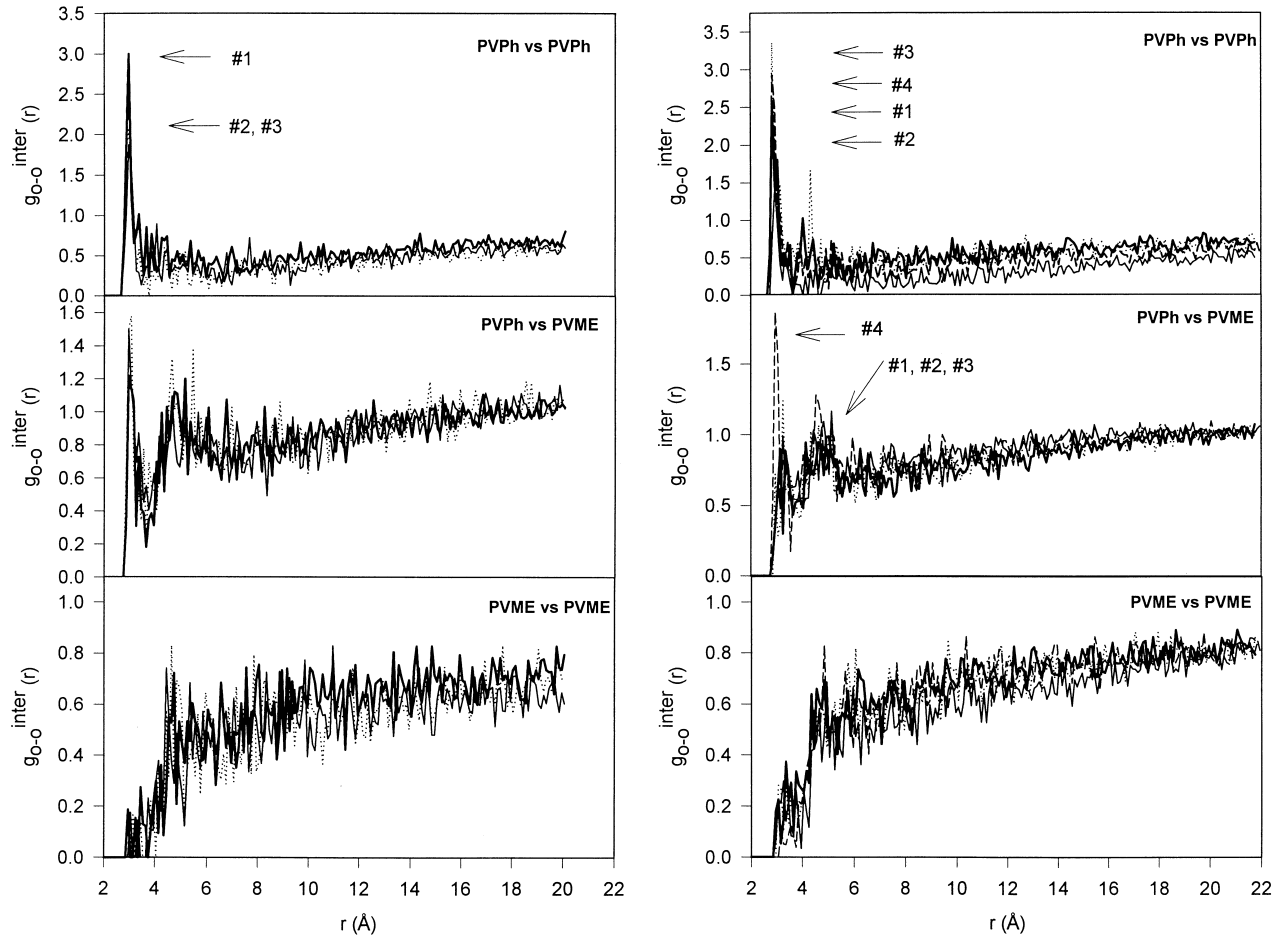

Fig. 6. Intermolecular distribution for the oxygen–oxygen pairs (thick line: Model 1, thin line: Model 2, dotted line: Model 3, dashed line: Model 4) (a) PP55 blends (b) PP37 blends.

very similar: high content in *trans* and *gauche* conformers are observed, whereas non-*trans*, non-*gauche* conformers, which have higher energies, occur in smaller proportion. Similarities between distributions for PVPh and PVME are not surprising, as their chain structure adopts the same general features: a main chain composed strictly of C–C bonds with a bulky side group present on every alternate carbon atom (phenyl alcohol for PVPh and methyl ether for PVME).

In blends, conformation distribution has not changed noticeably from that of the pure components. Therefore, for both components in the blend the most stable conformations (*trans* and *gauche*) prevail.

4. Conclusions

Simulation of miscible blends remains a challenge. Quantitative assessment of degree of interpenetration or intermingling is still difficult to correlate to experimental measurements. In the present work, a hydrogen bond forming blend was chosen and number of hydrogen bonds formed determined. Calculated solubility parameter and X-ray pattern were not found particularly useful to estimate the blend homogeneity in this specific case. Changes upon blending were observed in $g(r)$ and number of hydrogen bonds, and clearly show that the models have a good degree of intermingling, although it appears not to be uniform for all models. A clear correlation exists between energy and number of hydrogen bonds. The calculation of the pair correlation function for oxygen pairs proved to be a fast and useful tool for the qualitative assessment of hydrogen bonds in polymer systems.

Further work will be necessary to improve the models in terms of intermingling of the chains, for which various strategies could be attempted. These include varying the initial position of the chains as well as construction of models with shorter chains and higher number of chains. In such models, long enough NVT MD simulation times would allow diffusion through the system, improving the level of intermingling.

Acknowledgements

The authors wish to thank Professor J. Léonard for

helpful discussions and the referees for useful suggestions, in particular concerning $g(r)$ of oxygen atoms. This research was supported by the NSERC (National Science and Engineering Council of Canada), and by the FCAR (Fonds pour la Formation de Chercheurs et l'Aide à la Recherche). One of the authors, P. Gestoso, also acknowledges the support of the scholarships from the Ministère de l'Education du Québec and from Université Laval.

References

[1] Gestoso P, Brisson J. Polymer 2001;42:8415.
[2] Kremer K, Grest GS. J Chem Phys 1990;92:5057.
[3] Gao J, Weiner JH. Macromolecules 1996;29:6048.
[4] Barsky S, Slater GW. Macromolecules 1999;32:6348.
[5] Mavrantzas VG, Theodorou DN. Comp Theor Polym Sci 2000;10:1.
[6] Doxastakis M, Kitsiou M, Fytas G, Theodorou DN, Hadjichristidis N, Meier G, Frick B. J Chem Phys 2000;112:8687.
[7] Choi P, Blom HP, Kavassalis TA, Rudin A. Macromolecules 1995;28:8247.
[8] Clancy TH, Pütz M, Weinhold JD, Curro JG, Mattice WL. Macromolecules 2000;33:9452.
[9] Akten ED, Mattice WL. Macromolecules 2001;34:3389.
[10] Moskala EJ, Varnell DF, Coleman MM. Polymer 1985;26:228.
[11] Maple JA, Hwang M-J, Stockfisch TP, Dinur U, Waldman M, Ewig CS, Hagler AT. J Comp Chem 1994;15:162.
[12] Hwang M-J, Stockfisch TP, Hagler AT. J Am Chem Soc 1994;116:2515.
[13] Discover 3. Polymer 3.0.0, User Guide. San Diego: Biosym Technologies Inc., 1996.
[14] Gestoso P, Brisson J. Comp Theor Polym Sci 2001;11:263.
[15] Gestoso P, Brisson J. J Polym Sci, Part B 2002;14:1601.
[16] Shiomi T, Hamada F, Nasako T, Yoneda K, Imai K, Nakajima A. Macromolecules 1990;23:229.
[17] Arichi S, Himuro S. Polymer 1989;30:686.
[18] Ahmad H, Yaseen M. Polym Engng Sci 1979;19:858.
[19] Mason JA, Sperling LH. Polymer blends and composites. New York: Plenum Press; 1976.
[20] Brandrup J, Immergut EH, Grulke EA, editors. Polymer handbook, 4th ed. New York: Wiley; 1999.
[21] Lastoskie CM, Madden WG. In: Roe RJ, editor. Computer simulation of polymers. New Jersey: Prentice-Hall; 1991.
[22] Gestoso P, Nicol E, Theodorou DN, in preparation.
[23] Li D, Brisson J. Polymer 1998;39:793.